Lifetimes of SU(3) groups and ψ particles as a scaling in powers of α

Malcolm H. Mac Gregor
*Lawrence Livermore Laboratory, Livermore, California 94550**
(Received 23 December 1974; revised manuscript received 15 December 1975)

A study of the experimental systematics of elementary-particle lifetimes leads to the following conclusions: (a) Elementary-particle lifetimes τ divide empirically into two distinct groups—"particles" ($\tau > 10^{-21}$ sec) and "resonances" ($\tau < 10^{-22}$ sec), where "particle" lifetimes are spaced by powers of $\alpha = e^2/\hbar c$ and "resonance" lifetimes occur as a continuum of values; (b) the scaling of "particle" lifetimes in powers of α is a "lifetime democracy" in the sense that baryons, mesons, and leptons are all grouped together in one over-all lifetime scaling pattern; (c) integral-spin boson "particle" lifetimes scale in powers of α, whereas half-integral-spin fermion "particle" lifetimes scale in powers of α^2; (d) an SU(3) grouping of lifetimes reveals some striking patterns, with the ψ and ψ' lifetimes appearing as an extension of one of these patterns; (e) phase-space corrections, which are important for "resonance" lifetimes, are not as important for "particle" lifetimes; (f) if hadron lifetimes are grouped according to baryon number and strangeness, and then sorted into spin states, an empirical spin and lifetime correlation is seen in all of these groups: As the spin value increases, the maximum observed lifetime decreases.

I. EXPERIMENTAL SYSTEMATICS OF ELEMENTARY PARTICLE LIFETIMES

Recent experimental evidence indicates the existence of a number of massive and very-narrow-width resonances. Popularly referred to as the new particles, these include the J or $\psi(3095)$ particle,[1] the $\psi'(3684)$ particle,[2] some intermediate states of the ψ, ψ' system,[3] a possible heavy lepton,[4] and long-lived particles suggested by other experiments.[5] One of the most reliable methods for ascertaining the spectroscopic significance of these new particles is to compare their experimental properties to the experimental properties of the well-known particles.[6] The most distinctive experimental properties of the new particles are their large masses and their long lifetimes (narrow widths). However, a meaningful mass comparison is difficult to carry out,[7] since the masses of the new particles are much larger than the masses of the well-known particles. Thus we are left with new-particle lifetimes as the most meaningful spectroscopic quantities to examine from the standpoint of experimental comparisons.

There are 18 elementary particles, including the ψ and ψ' new particles, which have measured lifetimes $\tau > 10^{-21}$ sec, and there are approximately 138 meson and baryon resonances which have measured lifetimes $\tau < 10^{-22}$ sec (or widths $\Gamma > 6$ MeV). In the present section we first analyze the 18 long-lived particles, and we then extend these results to include the 138 short-lived resonances.

A. Lifetime ratios as factors of ten

The 18 elementary particles with measured lifetimes $\tau > 10^{-21}$ sec are listed in Table I.[1,2,6,8-11] Since the span of lifetimes shown in Table I is so large—24 orders of magnitude—physicists do not customarily group these particles lifetimes together in one category. Instead, the lifetimes $\tau > 10^{-16}$ sec are assigned to the domain of "weak" decays, the lifetimes $\tau < 10^{-16}$ sec are assigned to the domains of "electromagnetic" and "strong" decays, and these domains are treated separately.[12] If we now attempt to group these widely-spaced lifetimes together into one comprehensive picture, we are faced with the task of finding a meaningful framework that relates these domains to one another. Since our interest here is in relationships among lifetimes rather than in absolute lifetime values, it is convenient to set the lifetime of the longest-lived member of Table I, τ_{neutron}, equal to unity, and to express the other lifetimes of Table I as ratios $R_i = \tau_i/\tau_{\text{neutron}}$. The ratios R_i thus obtained are given in Table I. The lifetime τ_i of a particle can then be denoted by the parameter X_i, which is the logarithm of the ratio R_i to some suitably chosen base B, as follows:

$$\tau_i/\tau_{\text{neutron}} \equiv R_i = B^{X_i}, \tag{1}$$

where $B < 1$. The task of finding a suitable framework for studying elementary particle lifetimes thus becomes a matter of selecting an appropriate base B.

Figure 1 shows a plot of the lifetime parameters X for the 18 elementary particle lifetimes of Table I, using the logarithmic base $B = 10^{-1}$. As can be seen in the figure, this base appears to have no phenomenological significance. However, several lifetime groupings can be observed in Fig. 1, and the centroids of these groupings are separated by factors of roughly 10^2, or 100. This suggests that the base $\alpha \simeq 137^{-1}$ might be a suitable one to use for representing these lifetimes.

TABLE I. Experimental data on lifetimes for all elementary particles with $\tau > 10^{-21}$ sec. The experimental lifetime values are given, together with the ratios R of the lifetimes to that of the neutron [Eq. (1) in the text], and also the logarithms X of R to the base $\alpha = e^2/\hbar c$ [Eq. (2) in the text], including the experimental errors ΔX. Except as noted, all data are from RPP74, Ref. 6. A plot of the logarithms X is shown in Fig. 2.

Particle	Exp. lifetime τ (sec)	Lifetime ratio R	Logarithm X of R to the base α	Ref.
neutron	918 ± 14	1.0	$0.000 \pm (0.003)$	a
$\mu^{\pm}$	$2.1994 \pm 0.0006 \times 10^{-6}$	2.396×10^{-9}	4.034 ± 0.0001	
K_L^0	$5.179 \pm 0.040 \times 10^{-8}$	5.642×10^{-11}	4.796 ± 0.002	
$\pi^{\pm}$	$2.6030 \pm 0.0023 \times 10^{-8}$	2.836×10^{-11}	4.936 ± 0.0002	
$K^{\pm}$	$1.2371 \pm 0.0026 \times 10^{-8}$	1.348×10^{-11}	5.087 ± 0.0004	
Ξ^0	$2.96 \pm 0.12 \times 10^{-10}$	3.224×10^{-13}	5.846 ± 0.008	
Λ	$2.578 \pm 0.021 \times 10^{-10}$	2.808×10^{-13}	5.874 ± 0.002	
Ξ^-	$1.652 \pm 0.023 \times 10^{-10}$	1.800×10^{-13}	5.964 ± 0.003	
Σ^-	$1.482 \pm 0.017 \times 10^{-10}$	1.614×10^{-13}	5.986 ± 0.002	
Ω^-	$1.3^{+0.3}_{-0.2} \times 10^{-10}$	1.416×10^{-13}	$6.013^{+0.034}_{-0.042}$	
K_S^0	$0.886 \pm 0.007 \times 10^{-10}$	9.651×10^{-14}	6.091 ± 0.002	
Σ^+	$0.800 \pm 0.006 \times 10^{-10}$	8.715×10^{-14}	6.112 ± 0.002	
Σ^0	$\leq 1.0 \times 10^{-14}$	$\leq 1.1 \times 10^{-17}$	≥ 7.938	10
π^0	$8.21 \pm 0.43 \times 10^{-17}$	8.943×10^{-20}	8.914 ± 0.011	11
η	$7.74 \pm 1.09 \times 10^{-19}$	8.435×10^{-22}	$9.862^{+0.027}_{-0.031}$	8
$\psi(3095)$	$9.54 \pm 2.07 \times 10^{-21}$	1.039×10^{-23}	$10.756^{+0.040}_{-0.050}$	1
$\psi'(3684)$	$2.89 \pm 0.73 \times 10^{-21}$	3.144×10^{-24}	$10.999^{+0.045}_{-0.058}$	2
η'	$2.1^{+1.9}_{-0.7} \times 10^{-21}$	2.241×10^{-24}	$11.068^{+0.078}_{-0.129}$	9

[a] Zero neutron error was assumed in calculating errors for the logarithms X.

B. Lifetime ratios as factors of $\alpha = e^2/\hbar c$

The scaling of elementary-particle total or partial decay widths in powers of $\alpha = e^2/\hbar c$ has long been recognized for certain electromagnetic decays.[12] These decays involve a number n of photon interactions, with each interaction contributing a power of α, so that the factor α^n appears in the decay rate.[13] In the present section we extend this result to encompass all of the particles of Table I.

Figure 2 shows a plot of the lifetime parameters X for the 18 elementary particle lifetimes of Table I, using the logarithmic base $\alpha = e^2/\hbar c \approx \frac{1}{137}$; i.e.,

$$\tau_i/\tau_{\text{neutron}} \equiv R_i = \alpha^{X_i} . \tag{2}$$

In contrast to the lifetime parameters of Fig. 1,

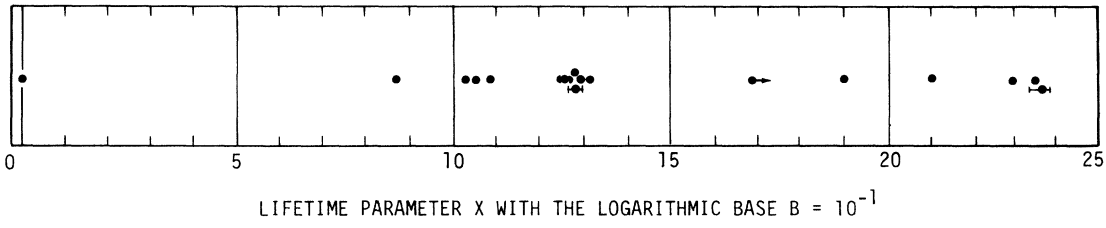

FIG. 1. The experimental lifetimes of Table I plotted along the abscissa as lifetime parameters X, using Eq. (1) in the text with the logarithmic base $B = 10^{-1}$. As can be seen in the figure, the base $B = 10^{-1}$ has no particular phenomenological significance; it is included here to provide a comparison to Fig. 2.

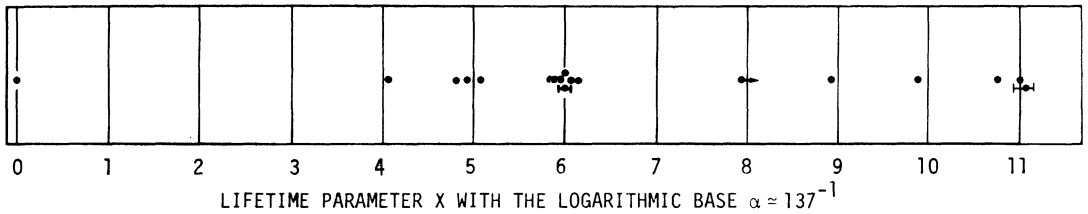

FIG. 2. This is the same plot as Fig. 1, but with the base $B = \alpha \simeq 137^{-1}$ [Eq. (2)] rather than the base $B = 10^{-1}$. When plotted in this manner, the lifetime parameters X exhibit a clear-cut integer periodicity. This indicates that the fine-structure constant $\alpha = e^2/\hbar c$ is a relevant scaling factor for these lifetimes.

the lifetime parameters of Fig. 2 exhibit a clear-cut integer periodicity, which indicates that the lifetimes scale as powers of α, with this scaling extending over the entire range of lifetimes included (the larger X values in Fig. 2 show a slight systematic shift to the left with respect to integer values, but this shift is consistent from one particle or group of particles to the next, so that the over-all periodicity in α is maintained).

Figure 3 is a detailed breakdown of the particle groups that were shown only as dots in Fig. 2. As can be seen in Fig. 3, we have a "lifetime democracy," with baryons, mesons, and leptons all fitting into the same α-spaced lifetime grid. This suggests that some universal type of decay mechanism must apply to all of these particles, and it indicates in particular that the so-called weak interaction is in some fundamental sense electromagnetic.

C. Statistical analysis of the lifetime scaling in powers of α

There are three methods we can use to establish the fact that the lifetime periodicity shown in Figs. 2 and 3 is not accidental:

(1) Demonstrated predictive power. The scaling of elementary-particle lifetimes in powers of α was first recognized[14] on the basis of the 14 particles in Table I which have lifetimes $\tau > 10^{-17}$ sec. Subsequent to the publication of this discovery,[14] the $\psi(3095)$ and $\psi'(3684)$ lifetimes appeared,[1,2] the $\eta(549)$ lifetime was revised upward by a factor of three,[8] and the $\eta'(958)$ lifetime was drastically revised upward.[9] All four of these lifetimes—ψ, ψ', η, η'—now fit into this previously established[14] scaling in powers of α, and they extend the scaling by two powers of α. We similarly expect other new particles[3-5] to fit into this same lifetime framework.

(2) Statistical probability. In Eqs. (1) and (2), the deviations ΔX of the lifetime parameters X from integer values can vary from $\Delta X = -0.5$ to $\Delta X = +0.5$. Figure 4 shows plots of the deviations ΔX for the 18 particles of Table I, where a whole series of logarithmic bases B in Eq. (1) are used, ranging from $B = \frac{1}{2}$ to $B = \frac{1}{1000}$. As can be seen in Fig. 4, a significant bunching of the deviations ΔX occurs only for values of B near $B = \frac{1}{137}$; for

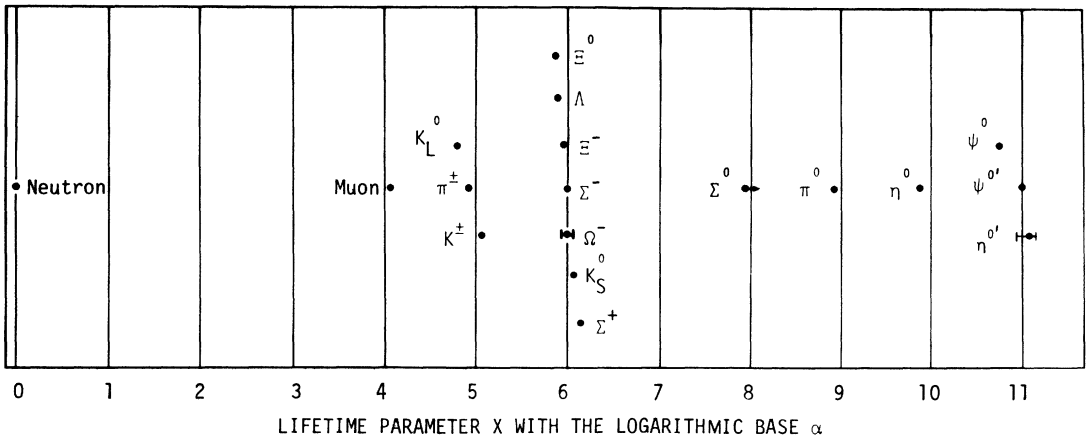

FIG. 3. This is the same plot as Fig. 2, but with the dots displaced vertically and labeled. As this figure reveals, we have a "lifetime democracy," with baryons, mesons, and leptons all combining together in one over-all lifetime pattern. The fact that the lifetimes of all 18 particles in Table I scale as powers of α (there are no counter-examples in this range) indicates that the so-called weak decays are in some fundamental sense electromagnetic.

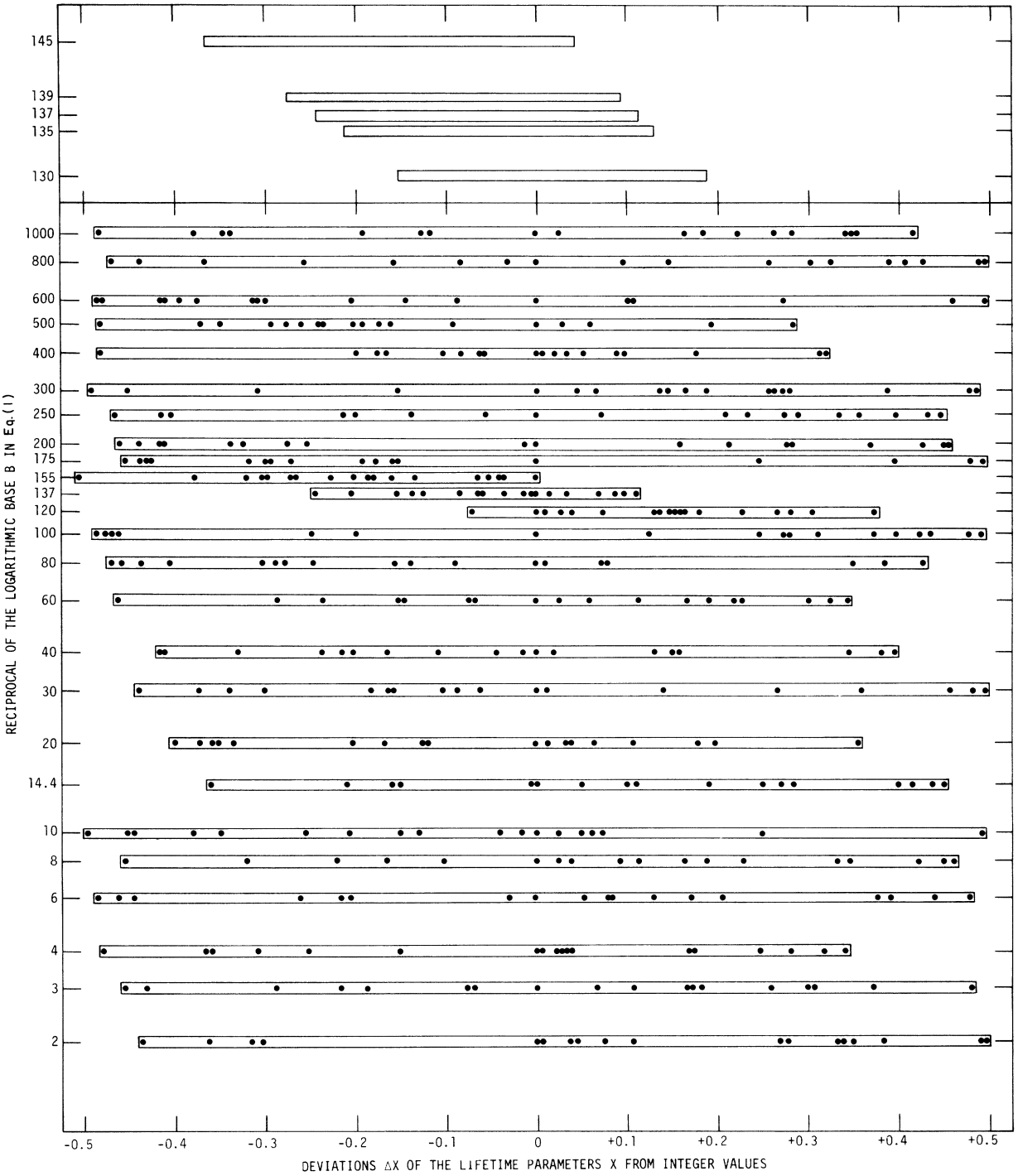

FIG. 4. This is an analysis of the logarithmic scaling of the 18 particle lifetimes in Table I. Equation (1) of the text was used together with a series of choices for the logarithmic base B, ranging from $B = \frac{1}{2}$ to $B = \frac{1}{1000}$. If the base B is relevant to the lifetimes, the deviations ΔX of the lifetime parameters X from integer values (or from some reference value) will be small; if the base B is not relevant, the deviations will be spread randomly from $\Delta X = -0.5$ to $\Delta X = +0.5$. As can be seen in Fig. 4, the ΔX values for the bases $B \ll \frac{1}{137}$ and $B \gg \frac{1}{137}$ are randomly spaced, whereas the ΔX values for $B \simeq \frac{1}{137}$ are compactly bunched. The ΔX envelopes shown at the top of Fig. 4 illustrate the detailed behavior of this bunching for values of B near $B = \frac{1}{137}$. As mentioned in the text, the compactness of this bunching for the base $B \simeq \frac{1}{137}$ arises from the fact that all 18 particles in Table I have lifetimes which scale in powers of α; there are no counter-examples.

other values of B, the deviations ΔX are spaced rather uniformly over the entire "deviation space," thus indicating random correlations. The deviations ΔX for $B \simeq \frac{1}{137}$ are concentrated in a sector that is just over $\frac{1}{3}$ of the available deviation space, thus indicating a significant correlation; from Figs. 2 and 3, these 18 lifetimes occur in 8 separate groups, so that the accidental probability for a bunching of this compactness is $(\frac{1}{3})^7 \sim 5 \times 10^{-4}$, where the base B is treated as a given (fixed) parameter, and where one group (the neutron) is used as a reference group. The smallness of this accidental probability stems of course from the fact that out of the 18 particles of Table I, there are no counter-examples to the observed scaling of lifetimes in powers of α; all 18 particles fit into this scaling pattern.

(3) Theoretical content. When the elementary particles of Fig. 3 are separated into SU(3)-suggested groupings, striking lifetime patterns emerge which reveal some of the underlying electromagnetic content of these particle lifetimes. It seems highly improbable that these patterns can be accidental.

Before delving into the theoretical sorting out of the lifetimes of Fig. 3, we first extend these results to include the lifetimes of the short-lived resonances.

D. The lifetime dichotomy of "particles" and "resonances"

Figure 2 is a plot of the lifetime parameters X for the long-lived particles of Table I, using the logarithmic base α [Eq. (2)]. Figure 5 is the same plot extended in X so as to include the short-lived (broad-width) resonances. These short-lived resonances are the approximately 138 resonances listed in the Review of Particle Properties[6] which have measured widths $\Gamma > 1$ MeV.[15]

The lifetime parameters X shown in Fig. 5 divide empirically into two quite different groups: (1) the long-lived particles which appear in the range $X = 0$–11 in Fig. 5, and which have lifetimes that are spaced by powers of α; (2) the short-lived particles which appear to the right of the arrow in Fig. 5 ($X \geq 11.7$), and which have essentially a continuum of lifetime values. It seems to be phenomenologically significant to distinguish between these two groups of particles. Hence in the present paper we denote these two groups as "particles" and "resonances," respectively, with the "particles" in the "particle region" having lifetimes $\tau > 10^{-21}$ sec and the "resonances" in the "resonance region" having lifetimes $\tau < 10^{-22}$ sec (widths $\Gamma > 6$ MeV). As Fig. 5 shows, the resonance region commences abruptly at the position of the arrow, and there is a gap of roughly one power of α between the particle region and the resonance region. The only resonance which appears in this gap is the ϕ meson.[16] The cutoff on lifetimes at $X \sim 12.6$ ($\Gamma \sim 600$ MeV) that is observed in Fig. 5 is due to lifetime limitations: the resonance must persist for a time that is longer than the transit time of the interaction.

From the many relationships which have been established among resonance widths on the basis of phase-space arguments, it seems clear that phase-space effects are important in the resonance region of Fig. 5; phase-space effects can lead to changes by factors of 10–100 in the observed decay widths,[12] and these phase-space effects are probably responsible for the continuum distribution of lifetimes in the resonance region. However, the accurate spacings in powers of α that are observed in the present paper for the *experimental* particle lifetimes indicate

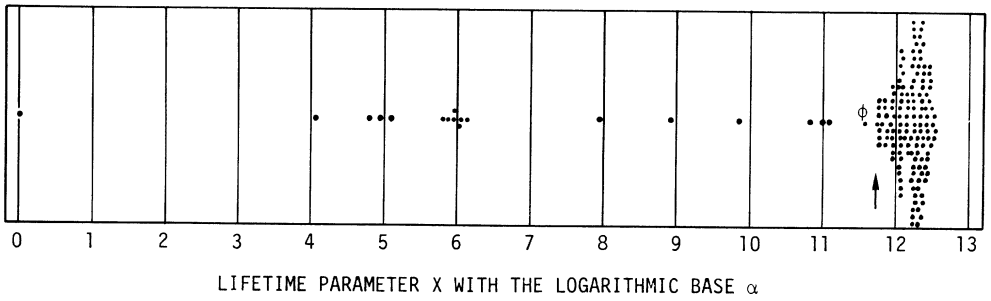

FIG. 5. This is Fig. 2 extended in X so as to include the approximately 138 short-lived resonances (Ref. 15) listed in RPP74 (Ref. 6). The ordinate is an evenly spaced distribution of lifetime parameters X after they have been sorted into $\Delta X = 0.1$ bins. As can be seen in the figure, the resonances in the resonance region (to the right of the arrow) commence abruptly at the position of the arrow, and they have essentially a continuum of lifetime values. This is in contrast to the particles in the particle region ($X \leq 11$), whose lifetimes are spaced by powers of α. The ϕ lifetime that is shown between these two regions is discussed in Ref. 16. The observed lifetime cutoff near $X = 12.6$ is a natural cutoff imposed by transit-time limitations.

that phase-space corrections in the particle region must be small; particles evidently have decays which are electromagnetically inhibited (as shown by the observed scaling in powers of α), and this inhibiting factor is essentially independent of the dictates of phase space. Phase-space corrections are discussed in detail in Sec. II.

E. The lifetime dichotomy of fermions and bosons

In Fig. 5, the lifetime parameters X of 18 particles and 138 resonances were plotted together. If we now make a separation of these 156 states into half-integral-spin fermions and integral-spin bosons, we obtain 88 fermion states—9 particles and 79 resonances—and 68 boson states—9 particles and 59 resonances. Figure 6 shows the results of plotting the fermion and boson states separately, using the same representation as in Fig. 5. As can be seen in Fig. 6, the fermion resonance region and the boson resonance region are essentially identical to one another. However, whereas boson particle lifetimes are separated from one another and from the boson resonance region by single powers of α, fermion particle lifetimes are separated from one another and from the fermion resonance region by powers of α^2. Hence we have phenomenologically related the number of virtual photons in the decay process[12] to the spin of the decaying particle, which is not a particularly surprising result.

Although the α-spaced lifetime grid of Figs. 2–6 is common to all types of elementary particles, the positions where "particles" appear on this grid seem to be determined by the type of decay process involved, as is shown by the breakdown

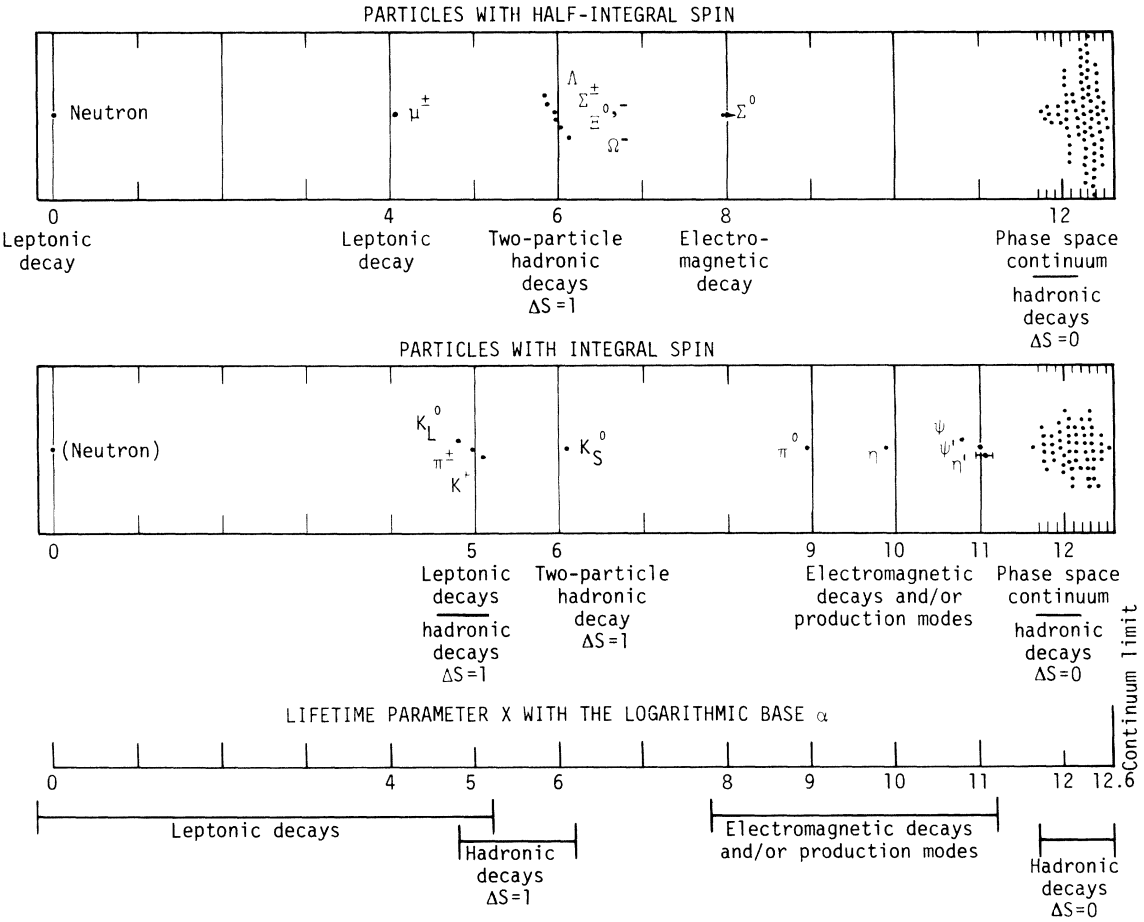

FIG. 6. This is a separation of the 156 particles and resonances of Fig. 5 into 88 half-integral-spin fermions (9 particles and 79 resonances) and 68 integral-spin bosons (9 particles and 59 resonances), using the same logarithmic plot and the same neutron reference lifetime for both fermions and bosons. As can be seen in the figure, the boson particle lifetimes are spaced by powers of α, whereas the fermion particle lifetimes are spaced by powers of α^2. The fermion and boson resonance regions are very similar to one another. The sorting out of the various types of decay modes which is shown at the bottom of this figure appears to be common to both fermions and bosons.

of decay modes given at the bottom of Fig. 6. This is further confirmation of the conjecture, stated above, that the long lifetimes of particles are due to characteristic electromagnetic inhibiting factors.

The separation of elementary particles into fermion and boson states has revealed some of the electromagnetic structure that is inherent in the decay processes of these particles (compare Figs. 5 and 6). This suggests that a further separation on the basis of spins and parities might reveal even more of this structure, a suggestion which is borne out by the results shown in Sec. I F.

F. SU(3) groupings of lifetimes

SU(3) classification schemes have demonstrated that when elementary particles are sorted out according to baryon number, spin, and parity, some very interesting isotopic spin regularities appear. This raises the question as to whether these same SU(3) selection rules also lead to interesting lifetime regularities. If we make an SU(3) breakdown of the 18 particle lifetimes in Table I, we obtain 7 baryon octet lifetimes (the proton is missing), one baryon decimet lifetime (the Ω^-), 7 pseudoscalar-meson lifetimes (the pseudoscalar nonet), two vector-meson lifetimes (the ψ and ψ'), and one lepton lifetime (the $\mu^\pm$). Figure 7 shows plots of the baryon lifetimes, including $J^P = \frac{1}{2}^+$ and $\frac{3}{2}^+$ SU(3) groupings, and Fig. 8 shows plots of the meson lifetimes, including $J^P = 0^-$ and 1^- SU(3) groupings. A plot of lepton lifetimes is also included in Fig. 8. The lifetimes in Figs. 7 and 8 are plotted on the same universal lifetime grid that was used for Figs. 2–6. We now discuss the plots of Figs. 7 and 8 in turn.

1. The baryons. Figure 7(a) is a plot of the lifetime parameters X for the 87 measured[15] baryon and hyperon states. This plot is very striking, both in its scope and in its simplicity. If we start with the neutron as a basic reference lifetime, a jump by a factor of α^6 (13 orders of magnitude) gives the lifetimes of the long-lived hyperon states, and a second jump by another factor of

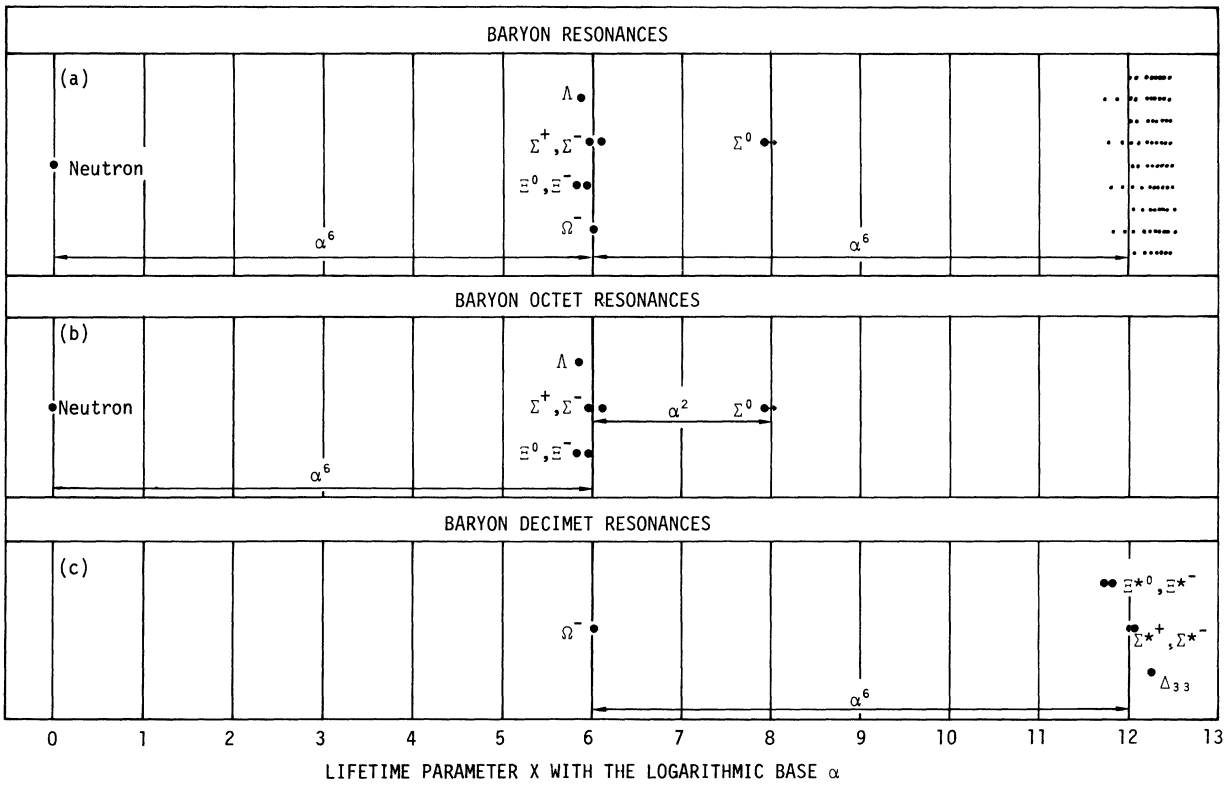

FIG. 7. Figure 7(a) is a plot of the 8 particle and 79 resonance hadron fermion lifetimes of Fig. 6. As can be seen, these divide into three main groups, which are separated from one another by factors of α^6. Figure 7(b) shows the baryon octet resonances (Ref. 6) from Fig. 7(a), and Fig. 7(c) shows the baryon decimet resonances (Ref. 6) from Fig. 7(a). In Fig. 7(b), the Σ^0 hyperon has a single-γ-ray electromagnetic decay which is not available to the other hyperons, and which evidently shortens its lifetime by a factor of α^2.

α^6 gives the lifetimes of the short-lived excited states in the baryon and hyperon resonance region.

If we now project relevant SU(3) groups out of the states in Fig. 7(a), we obtain the $J^P = \frac{1}{2}^+$ baryon octet lifetimes shown in Fig. 7(b) and the $J^P = \frac{3}{2}^+$ baryon decimet lifetimes shown in Fig. 7(c). Comparing Fig. 7(b) with Fig. 7(c), we see that the lifetimes of the octet and decimet groups are similar in that each group has one long-lived member which is separated from the shorter-lived members of the group by a factor of α^6; also, the octet and decimet lifetime groups are separated from one another by a factor of α^6.

The only exceptional cases are (1) the Σ^0 hyperon in Fig. 7(b), which has a single-γ-ray electromagnetic decay that evidently shortens the Σ^0 lifetime[10] by a factor of α^2, and (2) the proton, which is stable.

There is one ramification of the baryon lifetime systematics of Fig. 7 which is worth mentioning here. The two related jumps of α^6 which are shown in Fig. 7 constitute a total lifetime span of α^{12}, or 25 orders of magnitude. This is a much larger span than physicists are ordinarily accustomed to dealing with. Now the magnitude of the span between the electromagnetic and gravitational domains, which has always seemed to be

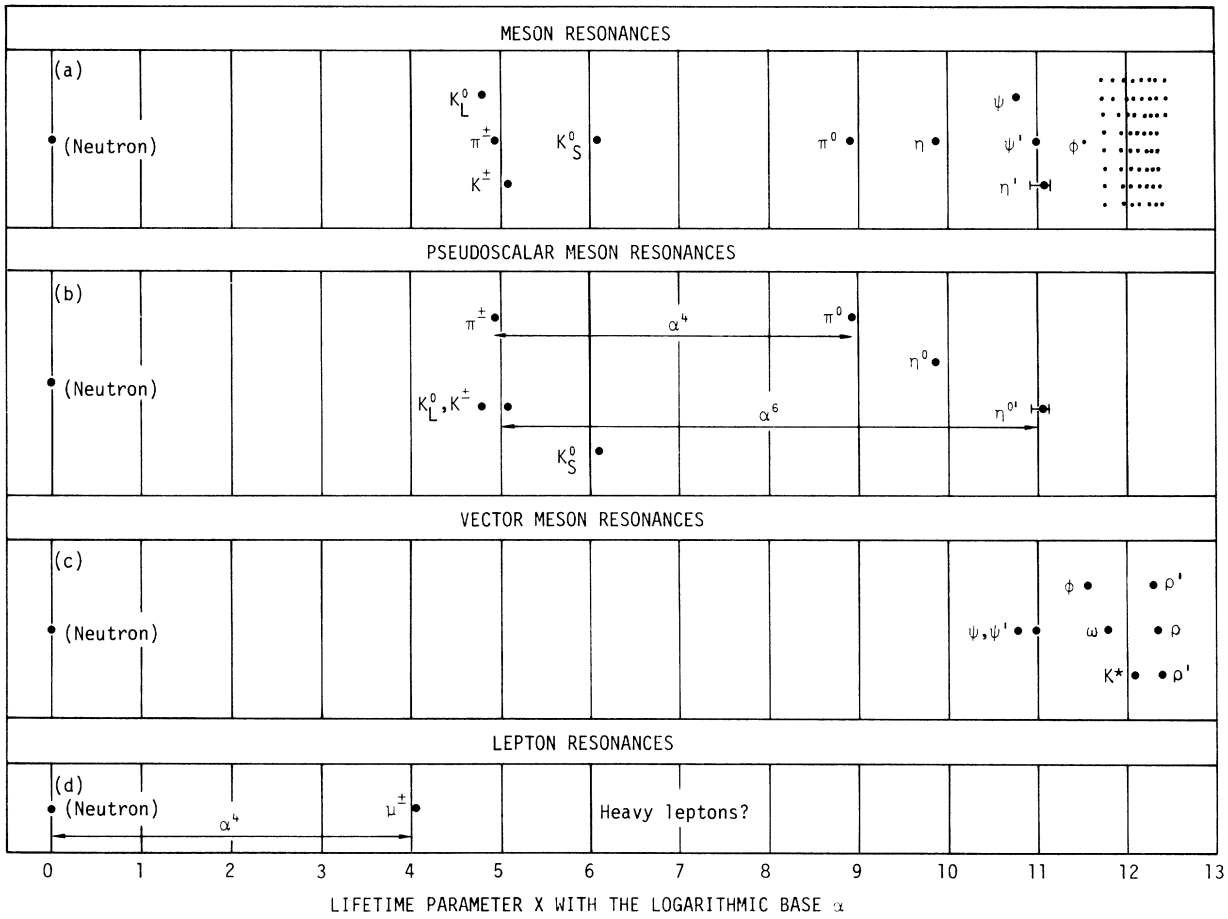

FIG. 8. Figure 8(a) is a plot of the 9 particle and 59 resonance boson lifetimes of Fig. 6. Figure 8(b) shows the spin-parity $J^P = 0^-$ pseudoscalar-meson states from Fig. 8(a), and Fig. 8(c) shows the $J^P = 1^-$ vector-meson states from Fig. 8(a). In Fig. 8(b), the π^0, η^0, and $\eta^{0\prime}$ mesons appear as a regularly spaced sequence, and the kaons form part of a similar sequence; the $(\pi^\pm - \pi^0)$ interval of α^4 (the π^0 has a double-γ-ray decay) echoes the $(\Sigma^\pm - \Sigma^0)$ interval of α^2 in Fig. 7(b) (the Σ^0 has a single-γ-ray decay); and $(K^\pm - \eta^{0\prime})$ interval of α^6 suggests that these particles may be related (see the α^6 intervals in Fig. 7, and see the discussion in the text). In Fig. 8(c), the ψ, ψ' lifetime group is displaced from the vector-meson resonance region by about one power of α, which suggests that the key to the unique properties of the ψ and ψ' is electromagnetic. Figure 8(d) is a lepton lifetime plot that is placed here for convenience. As can be seen in Fig. 8(d), the $(n - \mu^\pm)$ lifetime interval is just α^4 (see Ref. 20). If other heavy leptons are identified (see Refs. 4 and 5), it will be of interest to see where their lifetimes appear on the plot of Fig. 8(d).

so prohibitively large, is in fact just α^{18}. In view of the systematics of Fig. 7, this span of α^{18} may not be as totally impossible to bridge as we usually assume it to be.[17]

2. The pseudoscalar mesons. Figure 8(a) is the meson counterpart of the baryon plot of Fig. 7(a), and it shows the lifetime logarithms X for 68 measured[15] meson and kaon states. As can be seen in Fig. 8(a), the meson and kaon lifetimes are separated by single powers of α, which is in marked contrast to the α^2 and α^6 lifetime intervals observed in Fig. 7.

Seven of the lifetimes shown in Fig. 8(a)—$\pi^{\pm}$, π^0, η, η', $K^{\pm}$, K_L^0, and K_S^0—correspond to $J^P = 0^-$ spin-parity states.[6] These states, which are used to form the SU(3) pseudoscalar nonet,[6] are plotted together in Fig. 8(b). As can be seen in Fig. 8(b), the neutral meson states $\pi^0(135)$, $\eta^0(549)$, and $\eta^{0\prime}(958)$, which have successively increasing masses, also have lifetimes that are successively shorter by single powers of α. Similarly, the K_S^0 kaon state is separated from the K_L^0 and $K^{\pm}$ kaon states by one power of α.

We saw in Fig. 7(b) that the Σ^0 hyperon, which has a single-γ-ray electromagnetic decay, has a lifetime that is shorter than the Σ^+ and Σ^- lifetimes by a factor of α^2. Correspondingly, we see in Fig. 8(b) that the π^0 meson, which has a double-γ-ray electromagnetic decay, has a lifetime that is shorter than the $\pi^{\pm}$ lifetime by a factor of α^4.

It was demonstrated in Fig. 7 that related groups of strange and nonstrange states are characteristically separated by factors of α^6. Hence the observed separation of α^6 between the strange kaons and the nonstrange η' meson in Fig. 8(b) suggests that these states may be related. If we form the η' meson as a $K\bar{K}$ bound state, then the $\eta' = K\bar{K}$ system has a binding energy of 4%, which is precisely the same as the 4% binding energy observed *experimentally* by Gray *et al.*[18] for the $X^-(1795) = \bar{p}n$ meson bound state.[19]

3. The vector mesons. Figure 8(c) is a plot of the $J^P = 1^-$ spin-parity states from Fig. 8(a). Of these states, the ρ, ω, ϕ, and K^* constitute the SU(3) vector meson nonet,[6] the $\rho'(1250)$ and $\rho'(1600)$ are other recently identified vector mesons,[6] and the ψ and ψ' are new particles.[1,2] The lifetimes of the ρ, ω, K^*, $\rho'(1250)$, and $\rho'(1600)$ mesons (and possibly also the ϕ meson; see Ref. 16) lie in the meson resonance region. The ψ and ψ' lifetimes are shifted by one power of α from this resonance region. Hence they are analogous to the η' meson in Fig. 8(b), whose lifetime is also shifted by one power of α from the meson resonance region. While this does not constitute an "explanation" for the existence of the ψ and ψ' new particles, it indicates that their unique properties are electromagnetic in origin (which is hardly a surprise), and that the same underlying factor which is responsible for the single-power-of-α intervals observed in Fig. 8(b) is probably also responsible for the single-power-of-α interval observed in Fig. 8(c). Thus a theoretical explanation for the uniqueness of the ψ and ψ' particles should in some manner incorporate the fine-structure constant $\alpha = e^2/\hbar c$.

4. The leptons. The lepton lifetime plot, Fig. 8(d), is shown for convenience at the bottom of the meson lifetime plots. The $\mu^{\pm}$ is the only lepton with a measured lifetime,[6] and its lifetime falls rather suprisingly into the same lifetime grid that fits the baryons and mesons. The neutron-$\mu^{\pm}$ lifetime spacing of α^4 shown in Fig. 8(d) is a part of the general fermion lifetime systematics[20] of Fig. 6. There are also suggestions of other heavy leptons,[4,5] with lifetimes possibly in the general range indicated in Fig. 8(d). If these particles are clearly identified, it will be interesting to see where their lifetimes fall on the plot of Fig. 8(d).

G. A factor-of-two fine structure in "particle" lifetimes

Figure 9 is taken from Fig. 3; it shows the three $X \simeq 5$ lifetimes and the seven $X \simeq 6$ lifetimes plotted as relative lifetimes on an expanded logarithmic scale, with the seven $X \simeq 6$ lifetimes sorted out according to isotopic spin. As can be seen in Fig. 9, these supposedly independent particles have lifetimes that occur in accurate ratios of 1 : 2 and 1 : 2 : 4. These results have been published before[14]; they are repeated here because of their usefulness for studying phase-space corrections. As we show in Sec. II, these observed factors of two in the lifetime ratios *cannot* be attributed to phase-space effects, and the systematics of Fig. 9 in fact constitutes a powerful phenomenological tool for evaluating the accuracy of phase-space corrections as applied to lifetimes (total widths).

From the point-of-view of theories of elementary particle decays, the factor-of-two lifetime ratios shown in Fig. 9 may provide significant information.[21] However, it is beyond the scope of the present discussion to go into this matter. We merely note that (1) particle lifetimes empirically have a factor-of-two fine structure which is superimposed on an over-all scaling in powers of α; and (2) the $I = 0$ ψ and ψ' particles (see Fig. 3), whose lifetime ratio is 3.3 ± 1.1,[1,2] may or may not fit in with the systematics shown in Fig. 9.

II. PHASE-SPACE CORRECTIONS

The lifetime systematics displayed in Fig. 1–9 were obtained by working directly with the experi-

mental lifetimes, and not with phase-space-corrected lifetimes. The striking lifetime regularities noted for the particles in these figures indicate very directly that phase-space corrections to these lifetimes must be small (~20% or less). This is a fortunate circumstance, because in general it is impossible to correct particle total widths (lifetimes) for phase-space effects, owing to the different dimensionalities of the various final states. In the present section, we first sketch the manner in which phase-space corrections are applied, and we then show the results of applying (or trying to apply) these corrections to the particles of Fig. 3 and Table I.

A. Phase-space formalisms

Discussions of phase-space calculations are given, for example, in books by Feld[22] and Källén.[23] The transition probability λ_{fi} for going from a given initial state i of a particle to a given final state f is given by Fermi's "golden rule"[22]:

$$\lambda_{fi} = (2\pi/\hbar)|M_{fi}|^2\, dN_f/dE\,. \tag{3}$$

In cases where the transition matrix M_{fi} is slowly varying, the phase-space density dN_f/dE becomes the dominant factor in determining the distribution of the decay products f. Since particle wave functions, and hence particle transition matrix elements, are unknown, we are forced to use very general phenomenological considerations when we attempt to apply Eq. (3) to actual experimental situations. In particular, the accuracy of the assumption that the matrix element M_{fi} is constant over the region spanned by the final-state phase space can only be ascertained by the results to which this assumption leads in specific situations.

If the final state in Eq. (3) contains only two particles, the phase-space factor dN/dE has the simple form (in the barycentric system)[22]

$$dN(2)/dE = (V/2\pi^2)(p\epsilon_1\epsilon_2/E)\,, \tag{4}$$

where V is the normalization volume, p is the linear momentum of either particle, ϵ_1 and ϵ_2 are the particle energies, and E is the energy of the decaying resonance. If the decay products are all strongly interacting hadrons, then the normalization volume is sometimes replaced by the short-ranged interaction volume v, where $v \propto (\hbar/mc)^3$, with m being a characteristic mass for the reaction. This gives

$$dN(2)/dE \propto [(\hbar/mc)^3/2\pi^2](p\epsilon_1\epsilon_2/E) \tag{5}$$

for the two-particle final state of Eq. (4). If the final state contains three particles, then dN/dE can be handled analytically only in the cases where all three particles are either nonrelativistic or else highly relativistic. These two limiting cases give[22]

$$dN(3)/dE = 4\pi^3[V^2/(2\pi)^6] \times [m_1 m_2 m_3/(m_1+m_2+m_3)]^{3/2}Q^2 \tag{6}$$

and

$$dN(3)/dE = (7\pi^2/240)[V^2/(2\pi)^6]E^5\,, \tag{7}$$

respectively, where m_i are the masses of the nonrelativistic final-state particles, Q is the reaction energy, and E is the total energy of the resonance.

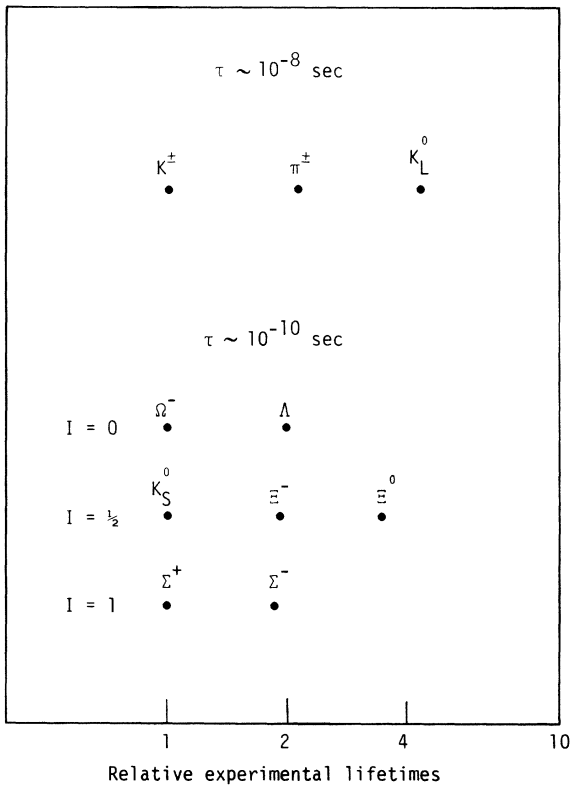

FIG. 9. This is a logarithmic plot of the relative experimental lifetimes for the three particles observed near $X = 5$ ($\tau \sim 10^{-8}$ sec) and for the seven particles observed near $X = 6$ ($\tau \sim 10^{-10}$ sec) in Figs. 2 and 3. The three $\tau \sim 10^{-8}$ lifetimes occur in the ratio 1:2:4, which is surprising for these supposedly independent particles. The seven $\tau \sim 10^{-10}$ lifetimes, when sorted out according to isotopic spin, also exhibit factor-of-two lifetime ratios, which indicates that these results are not accidental. If phase-space corrections are applied (see Fig. 11), the (Ξ^-, Ξ^0) and (Σ^+, Σ^-) pairs shift slightly to even more accurate 1:2 lifetime ratios (see Eq. 10 in the text). This indicates two things: (1) the factors of two shown in this figure do *not* arise from phase-space considerations; and (2) phase-space corrections, if properly applied, are probably small for all of the particles shown in Fig. 9.

Equation (6) is applicable to $K \to \pi\pi\pi$ decays, and Eq. (7) is applicable to the $\mu \to e + \nu + \bar{\nu}$ decay.

By comparing Eq. (4) with Eqs. (6) and (7), we can see an immediate difficulty if we attempt to apply phase-space corrections to total widths, and hence to lifetimes. The η meson, for example, decays 38% of the time into $\gamma\gamma$, which is a two-particle final state, and 54% of the time into $\pi\pi\pi$, which is a three-particle state. The phase-space correction for the $\eta \to \gamma\gamma$ decay involves the normalization volume V, and the correction for the $\eta \to \pi\pi\pi$ decays involves V^2. Thus the ratio of these two corrections depends on the normalization volume V, which of course is a completely unphysical situation. The only way out of this dilemma is to assign to V a specific value that comes from physical considerations, and the only logical choice here is to replace V by the interaction volume v, as we did in going from Eq. (4) to Eq. (5). However, the effective interaction radius is not known to better than a factor of two or three (for example, on p. 68 of Ref. 12 Feld suggests the pion Compton wavelength; and on p. 158 of Ref. 12 he suggests a radius $\hbar/mc$, with $m = 335$ MeV), so that the effective interaction volume v is not known to better than an order of magnitude. Hence there is no meaningful way that we can correct lifetimes for phase-space effects if the final states are of different dimensionalities. Furthermore, even if two final states have the same dimensionality, they may still have quite different effective interaction radii (e.g., $K^{\pm} \to \mu + \nu$ and $K^{\pm} \to \pi\pi$). The final states may also contain different spin factors. As a result of these intrinsic difficulties, the only way to judge the significance of making phase-space corrections to lifetimes (total widths) is the operational procedure of applying the corrections and seeing what happens.

In addition to the difficulties just discussed, there is some arbitrariness in the choice of equations to be used for representing phase-space effects. The transition amplitudes can be written in the form of Eqs. (4)–(7) above, which are not covariant and hence must be used only in the center-of-mass system,[22] or they can be written in a covariant form, as described for example in RPP74.[6] Also, there is some choice as to whether certain energy-dependent factors should be left in the transition matrix elements or else removed and added to the phase-space factors. If we go over to a covariant form for the transition matrix elements, the factors d^3p_i are replaced by d^3p_i/ϵ_i in the density-of-states term, which removes the factors ϵ_1 and ϵ_2 from Eq. (4). Also, in RPP74 a factor of E^{-1} is removed from the transition matrix element. Thus, for *meson* resonances, the RPP74 two-body transition probabilities are of the form

$$\lambda \sim |M|^2 (p/E^2), \tag{8}$$

in the notation of Eqs. (3) and (4). For baryon decays to baryon plus meson, the spin terms supply an extra factor of E, so that for the *baryon* decays, the RPP74 two-body transition probabilities are of the form

$$\lambda \sim |M|^2 (p/E). \tag{9}$$

The above discussion has been centered on the phase-space factor dN_f/dE in Eq. (3). However, the matrix element M_{fi} in Eq. (3) also merits some discussion. If we study Eq. (3) from the point of view of the experimental-particle decay rates, it seems clear that the large differences observed between the very slow (inhibited) decays and the fast (strong) decays must be due to fundamentally different decay mechanisms, and not to phase–space factors. Since phase-space factors dN/dE can change by factors of 10–100 in going from one resonance to another, we can account for variations in λ by factors of 10–100 as arising from phase-space effects,[12] but we cannot account for variations by factors of 10^{10} or so in this manner. For example, the $J^P = 1^-$ meson resonances $\rho(770) \to \pi\pi$ and $\omega(783) \to \pi\pi\pi$ have lifetimes $\tau \sim 4 \times 10^{-24}$ sec and $\tau \sim 6 \times 10^{-23}$ sec, respectively, and the factor of 15 difference in their lifetimes is logically attributed to the difference between 2π and 3π final-state phase-space volumes. But if we now compare $\rho(770) \to \pi\pi$ with $K_S^0(498) \to \pi\pi$, we find lifetimes $\tau \sim 4 \times 10^{-24}$ sec and $\tau \sim 1 \times 10^{-10}$ sec, respectively, which is a lifetime ratio of more than 10^{13}. This large a difference in the lifetimes cannot be attributed to phase-space or spin effects. The K_S^0 decay is inhibited, and the inhibiting factor (strangeness and/or parity) must be in the matrix element M_{fi} and not in the phase-space factor dN/dE. From this viewpoint, it seems reasonable that the matrix elements M for all of the resonances in the resonance region of Figure 5 (to the right of the arrow) do not contain inhibiting factors, and the matrix elements M for all of the particles in the particle region of Figure 5 (the region $X \leq 11$) do contain (electromagnetic) inhibiting factors. In particular, the ψ and ψ' resonances, which stand at the boundary between these two regions, are clearly inhibited, since otherwise their large mass values would lead to very rapid decays. If the matrix elements M differ discontinuously in these two regions, then the validity of the way in which phase corrections can be applied may also differ. Empirically, as we have already discussed, the total widths of the resonances appear to be responsive to the dictates of phase space, whereas the total

widths of the particles are not. This leads to the conclusion that the "inhibiting factors" in the particle matrix elements are essentially independent of phase-space considerations.

There is another viewpoint that we can use in studying phase-space corrections. These corrections are based in essence on the Gibbsian assumption that the hadronic interaction has a statistical distribution of final-state momenta. Now the ω meson, for example, has a lifetime $\tau \sim 6 \times 10^{-23}$ sec, so that the ω resonance persists for a distance of about 18 F (where we ignore any special-relativistic distortions). Thus the ω stays together for a distance that is about ten times the "length" of the interacting particles, and then breaks up. Hence it seems plausible that this relatively brief existence will be strongly influenced by statistical considerations. This result is even more true for the ρ meson, which persists for a distance of about 1 F; the ρ breaks up essentially as soon as it is formed, and statistical considerations must be all important in such a case. However, the $\pi^{\pm}$ meson, for example, which persists for a distance of about 8 m, is a stable particle in comparison to the ρ and ω mesons, and there is no reason to assume that the factors which lead to its eventual decay bear any resemblance at all to the Gibbsian statistical production and decay mechanisms which obtain for the ρ and ω mesons.

B. Phase-space applications

The seven particles clustered near $X = 6$ in Fig. 3 are the only particles which decay primarily into two-hadron final states; hence these are the only particles to which phase-space corrections can be applied with any degree of confidence. The $\pi^{\pm}$, Σ^0, and π^0 particles in Fig. 3 also have decays into two-particle final states, but the final-state particles for these decays are not both hadrons, so that the effective volumes for the decay interactions may vary from decay to decay. The other particles in Fig. 3 either have three-particle final states or else have a mixture of two-particle and three-particle final states, so that phase-space corrections for the total widths of these particles either are difficult to compare with the corrections for the two-particle decays just described or else are essentially impossible to apply at all.

If we confine our attention to the particles in Fig. 3 which have two-body decays, then we should use a particle such as the Σ^- for a reference lifetime, since the neutron has a three-body decay mode. Figure 10 shows the results of applying phase-space corrections to these particles. We first apply Eq. (4), with the normalization volumn V kept the same for all decays. As is shown in the middle row in Fig. 10, these phase-space corrections have only a small effect on the lifetimes near the logarithm $X = 0$ (which was the logarithm $X = 6$ in Fig. 3), but they shift the $\pi^{\pm}$, Σ^0, and π^0 lifetimes so as to destroy the scaling in powers of α. Since these last three lifetimes are for decays which include particles that are not hadrons, the interaction volumes for these decays may be different from the interaction volumes for the particles near $X = 0$. To investigate this possibility, we next apply Eq. (5) to these same lifetimes, with the interaction volume now set proportional to $(\hbar/mc)^3$, where m is the mass of the decaying particle. As is shown in the bottom row in Fig. 10, the scaling of lifetimes in powers of α is again destroyed. [In these last results, we have also included a corrected lifetime for the $\mu^{\pm}$ meson, which has a three-body final state, by using Eq. (7) for the correction.] Finally, if we apply the covariant correction factors of Eqs. (8)

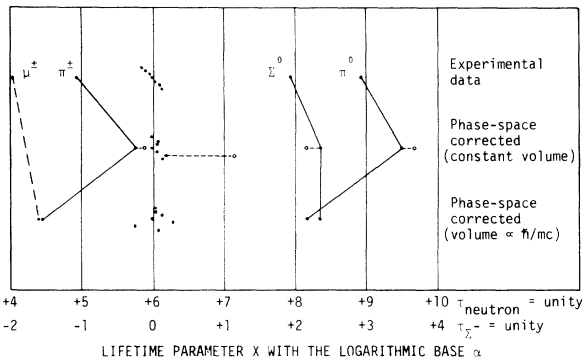

FIG. 10. Phase-space corrections as applied to some of the particle lifetimes of Fig. 3. The ten particles shown in the top row of Fig. 10 (excluding the $\mu^{\pm}$) all have two-body decays, so that their phase-space corrections have the same dimensionality and hence can be intercompared. The Σ^- lifetime, which corresponds to a two-body decay, was used as the reference lifetime for this intercomparison. Applying Eq. (4) in the text with the normalization volume V kept the same for all particles gave the corrected lifetimes shown in the middle row of Fig. 10, and applying Eq. (5) with V proportional to the Compton wavelength gave the results shown in the bottom row [Eq. (7) was used for the $\mu^{\pm}$ meson in the bottom row]. Applying the covariant phase-space corrections of Eqs. (8) and (9) gave results similar to those of Eq. (4) (except for the K^0_S meson); some of these corrections are indicated by the small open circles in the middle row of Fig. 10. As can be seen in the figure, the seven particles near $X = 0$ ($X = 6$), which all have two-hadron final states, are only mildly affected by the phase-space corrections, whereas the lifetimes of the other particles, which have nonhadronic final states, are shifted radically so that the scaling in α is destroyed.

and (9), we obtain results which are very similar to the results obtained by using Eq. (4); these results are partially illustrated by the small circles shown in the middle row of Fig. 10. The main difference between using Eq. (4) and using Eqs. (8) and (9) is that in the latter case the K_S^0 meson, owing to its different energy dependence (Eq. 8) from that [Eq. (9)] of its $X=0$ neighbors, is shifted to the right by about one power of α. Once again, applying these phase-space correction factors destroys the observed scaling of lifetimes in powers of α.

From a visual inspection of Fig. 3, it seems intuitively clear that the observed correlation between particle lifetime ratios and the fine-structure constant $\alpha = e^2/\hbar c$ must be physically significant. If this conclusion is correct, then the fact that the phase-space corrections shown in Fig. 10 destroy this scaling in powers of α must mean that these corrections were not properly applied. We can investigate this possibility by studying in detail the seven particles in Fig. 3 which are grouped together near $X=6$, since these are the particles for which phase-space corrections can be most reliably applied. The effect of applying phase-space corrections to these seven particles, which was shown on a compressed scale in Fig. 10, is shown on an expanded scale in Fig. 11 (which is a plot analogous to that of Fig. 9). Phase-space corrections are applied with the most reliability to the Σ^-, Σ^+ and Ξ^0, Ξ^- pairs in Fig. 11, and it can be seen there that the ratios of these pairs of lifetimes remain essentially constant as corrections based on Eqs. (4), (5), and (9) are successively applied. The Λ/Ω^- lifetime ratio, on the other hand, changes somewhat with the various phase-space corrections. Two possible reasons for this change are that the spin of the Ω^- is not known and that the $\Omega^- \to \Xi\pi$ and $\Omega^- \to \Lambda K$ decays, which have considerably different phase-space corrections, have an unknown branching ratio (in making the Λ/Ω^- corrections shown in Fig. 11, a branching ratio of $\frac{1}{3}$ to $\frac{2}{3}$ was assumed, and spin differences were ignored). The Ξ^-/K_S^0 phase-space correction is expected to be the most uncertain since the Ξ^- is a spin-$\frac{1}{2}$ baryon and the K_S^0 is a spin-0 meson, and as can be seen in Figs. 10 and 11 the Ξ^-/K_S^0 lifetime ratio varies wildly as Eqs. (4) and then (5) and then (8) and (9) are successively applied.

If we now compare Fig. 11 with Fig. 9, we can by inference draw some rather powerful general conclusions about phase-space corrections for particles. In the only two cases in Fig. 11 where the phase-space corrections are known to be reliable, namely in the lifetime ratios Σ^-/Σ^+ and Ξ^0/Ξ^-, the corrections turn out to be small. In

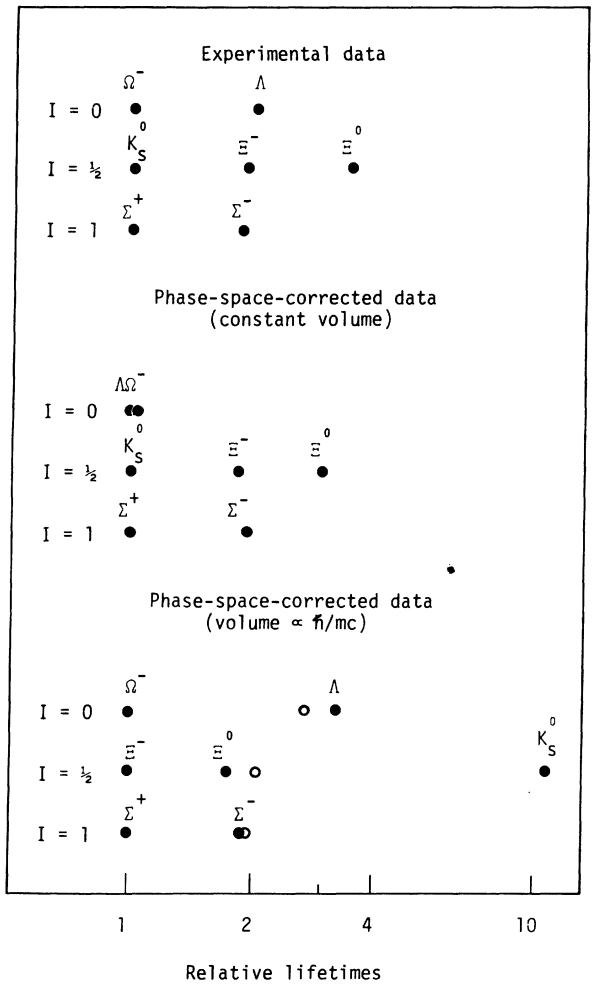

FIG. 11. The effect of applying phase-space corrections to the seven particles near $X=6$ in Fig. 3, which all have two-hadron final states. The experimental data at the top of Fig. 11 are from Fig. 9. The constant-volume corrections of Eq. (4) are shown in the middle row of Fig. 11, and the Compton-wavelength-normalized corrections of Eq. (5) are shown in the bottom row. The covariant corrections of Eq. (9) are indicated by the open circles in the bottom row (the effect of Eqs. 8 and 9 on the K_S^0/Σ^- ratio is illustrated in Fig. 10). The stability of the (Ξ^-, Ξ^0) and (Σ^+, Σ^-) pairs indicates that phase space is *not* responsible for the observed factor-of-two lifetime ratios; this indicates in turn that the observed factors of two in the (Ω^-, Λ) and (K_S^0, Ξ^-) experimental lifetime ratios are probably physically significant, and that the phase-space corrections calculated here for these particles are not quantitatively reliable (they should be small corrections). Thus we conclude that, with our present theoretical limitations, experimental lifetimes rather than "phase-space-corrected" lifetimes are the proper quantities to study for the particles of Fig. 3.

particular, if we apply the most reliable phase-space correction to these ratios—namely Eq. (9), which is covariant and contains the proper spin factors—we obtain the following results:

Lifetime ratio	Experimental	Corr. by Eq. (9)
Σ^-/Σ^+	1.85	1.90
Ξ^0/Ξ^-	1.79	2.05

(10)

These results are crucial to the present discussion, because when they are applied to the systematics of Figs. 11 and 9, they lead to the following chain of conclusions:

(1) The factors of two shown in Eq. (10) for the phase-space-corrected Σ^-/Σ^+ and Ξ^0/Ξ^- lifetime ratios must be physically significant.

(2) These factors of two must be inherent in the (covariant) transition matrix elements $|M|^2$, and not in the phase-space factors dN/dE, so that the observed factor-of-two lifetime ratios are *not* a phase-space effect.

(3) If the factors of two observed for the Σ^-/Σ^+ and Ξ^0/Ξ^- lifetime ratios in Fig. 9 are physically significant, then all of the other factors of two shown in Fig. 9 are probably physically significant, and they should likewise be attributed to factors in the matrix elements rather than to phase-space factors.

(4) Conclusion (3) suggests in turn that the phase-space corrections to all of the particles in Fig. 9, if properly applied, must be small, since the experimental lifetime ratios are very nearly factors of two.

(5) If we carry the factor-of-two line of reasoning of Fig. 9 over to Fig. 3 and apply it to the observed factors of α, we can at least tentatively conclude that phase-space corrections for all of the particles of Fig. 3 must be small (which implies that the "electromagnetic lock" on the decay modes of each of these particles is independent of phase-space considerations).

(6) The above results indicate that the large phase-space corrections shown in Figs. 10 and 11 for the $\mu^\pm$, $\pi^\pm$, Ω^-, K_S^0, Σ^0, and π^0 lifetimes are not meaningful. In particular, the large fluctuations observed for the phase-space-corrected lifetimes of these particles as we go from Eqs. (4)

TABLE II. A list of the 74 hadrons whose spins and lifetimes (or widths) are described in RPP74, Ref. 6, as being well known. [a] Although sorted here into spin states, the mesons and kaons follow the listing order on p. 8 of RPP74, and the baryons and hyperons follow the listing order on p. 10. The lifetime or width values used for the plot of Fig. 12 are the averages quoted in RPP74.

Mesons (24):	($J=0$)	$\pi^0, \pi^+, \eta, \epsilon, \eta', \delta, S^*$
	($J=1$)	$\rho, \omega, \varphi, A_1, B, \rho', D, \rho', E, \psi$ (or J), ψ'
	($J=2$)	f, A_2, f', A_3
	($J=3$)	g
	($J=4$)	h
Kaons (8):	($J=0$)	$K^\pm, K_L^0, K_S^0, \kappa$
	($J=1$)	K^*, Q
	($J=2$)	K^*, L
Baryons (19):	($J=\frac{1}{2}$)	$p, n, N(1470, 1535, 1700, 1780)$, $\Delta(1650, 1910)$
	($J=\frac{3}{2}$)	$N(1520, 1810)$, $\Delta(1232, 1670)$
	($J=\frac{5}{2}$)	$N(1670, 1688)$, $\Delta(1890)$
	($J=\frac{7}{2}$)	$N(2190)$, $\Delta(1950)$
	($J=\frac{9}{2}$)	$N(2220)$
	($J=\frac{11}{2}$)	$\Delta(2420)$
Hyperons (23):	($S=-1$) ($J=\frac{1}{2}$)	$\Lambda, \Lambda(1405, 1670)$, $\Sigma^+, \Sigma^0, \Sigma^-, \Sigma(1750)$
	($J=\frac{3}{2}$)	$\Lambda(1520, 1690)$, $\Sigma(1383, 1387, 1670, 1750)$
	($J=\frac{5}{2}$)	$\Lambda(1815, 1830)$, $\Sigma(1765, 1915)$
	($J=\frac{7}{2}$)	$\Lambda(2100)$, $\Sigma(2030)$
	($S=-2$) ($J=\frac{1}{2}$)	Ξ^0, Ξ^-
	($J=\frac{3}{2}$)	$\Xi^0(1532)$, $\Xi^-(1535)$

[a] The only ambiguous states included here, the D and E mesons (see Ref. 24) and the L kaon, have been assigned their most probable spin values. The ψ (or J) and ψ' mesons are from Refs. 1 and 2, and the h is from Ref. 25.

to (5) to (8) and (9) are an indication that the magnitude of the correction depends in an essential way on (unknown) normalization factors, and conclusions (1)–(5) suggest that with properly chosen normalizations the phase-space corrections would in fact be small.

Hence, for the particles of Figure 3, we are forced back to experimental lifetimes as the most meaningful quantities to study from the point of view of the present systematics.

III. AN EMPIRICAL CORRELATION BETWEEN SPINS AND LIFETIMES

Up to this point, we have been discussing the manner in which elementary-particle lifetimes scale in powers of α. There is one additional lifetime result which does not relate directly to this scaling in α, but which should be included here for completeness. In Sec. IF, we grouped particle lifetimes into SU(3)-suggested J^P spin and parity groups. If we instead group lifetimes into baryon number B and strangeness S groups, and then sort these (B,S) groups into spin states J, we discover an empirical relationship between spins and lifetimes: the higher the spin, the shorter the maximum observed lifetime.

Table II lists the 74 hadron states for which the spins and the lifetimes (or widths) have been reliably determined.[1,2,6,24,25] If we plot the lifetimes of these 74 states in (B,S) groups, using the same universal lifetime grid as in Figs. 2–8, we obtain the results shown in Fig. 12. The dots in Fig. 12 are the lifetime parameters X, and the envelopes surrounding the dots denote the range of lifetime values observed in each (B,S,J) state. Within each (B,S) group, the maximum observed lifetime (the minimum value of X) increases as the spin J decreases. In particular, the 14 particles with long lifetimes ($\tau > 10^{-20}$ sec) occur in the lowest possible spin states, $J=0$ and $J=\frac{1}{2}$. The only exception to this empirical result is the $S=-3$ Ω^- hyperon, whose spin has not been determined experimentally as yet,[26] but which is identified on

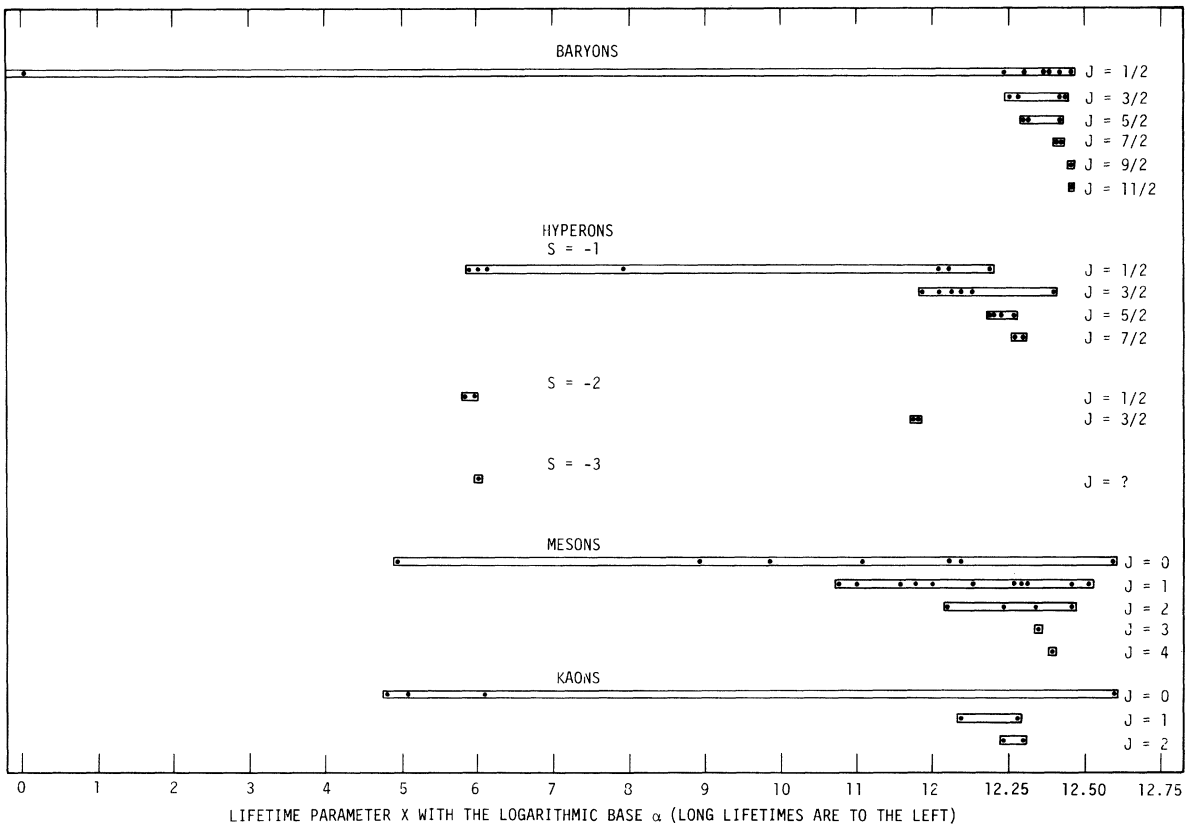

FIG. 12. The lifetime parameters X [Eq. (2)] for the particles in the hadron families of Table II, using the logarithmic base α [Eq. (2)]. The dots denote the parameters X, and the envelopes surrounding the dots indicate the range of experimental lifetimes observed in each spin state J (note the expanded scale for $X > 12$). As can be seen, there is a well-defined correlation in each family between the spin and the maximum observed lifetime (the minimum value of X). The Ω^- hyperon, whose spin has not been measured, is included here for comparison purposes.

the basis of SU(3) symmetries as a spin $J = \frac{3}{2}$ resonance. The lifetime of the Ω^- is $\tau = 1.3 \times 10^{-10}$ sec, whereas the lifetimes of the 12 known $J = \frac{3}{2}$ hadrons in Fig. 12 are all less than 10^{-22} sec (the quantum numbers of the Ω^- prevent it from having a strong decay).

IV. CONCLUSIONS

Although the lifetime regularities displayed in Figs. 2–12 lead to many ramifications, as noted throughout the text, the principal conclusions with respect to the present discussion seem to be the following:

(1) All particles—leptons, mesons, and baryons—appear in the lifetime systematics on an essentially equal footing, so that there must be some underlying theory which includes all of them (in contrast to many of the present-day hadron theories, for example, which have no place to include the muon).

(2) The observed lifetime scaling in powers of α extends uniformly throughout the regions of both "weak interactions" and "electromagnetic interactions," so that the so-called weak interaction must in some fundamental sense be electromagnetic, and the fine-structure constant α should appear in theories of weak interactions.

(3) There appears to be a real lifetime dichotomy of particles and resonances: resonances have fast decays that depend strongly on phase space; particles have electromagnetically inhibited decays that depend only weakly on phase space.

(4) Half-integral-spin fermion decays involve only even powers of α, whereas integral-spin boson decays include odd powers of α.

(5) The same SU(3) spin-parity-baryon number groupings which lead to striking isotopic spin regularities also lead to striking lifetime regularities.

(6) The ψ and ψ' new particles constitute a new type of lifetime group, but one that fits into and extends the lifetime patterns of the SU(3) groups.

(7) The key to the special qualities of the ψ and ψ' new particles (that is, their unique combinations of large masses and long lifetimes) must be electromagnetic in nature, so that the constant α should logically appear in new-particle theories.

Note added in proof. There is an important point to be brought out in connection with the spin versus lifetime relationship shown in Fig. 12. In nuclear physics, centrifugal-barrier effects lead to the result that resonances with high spin values have narrow widths (long lifetimes). In Fig. 12, however, we see just the opposite situation—resonances with high spin values have broad widths (short lifetimes). This indicates that centrifugal-barrier effects (see Ref. 6, p. 194) do *not* apply in the same manner to these elementary-particle resonances. This result can be understood by noting that nuclear rotations are adiabatic, so that the over-all central potential (to which the centrifugal-barrier term is added) is not appreciably affected by the rotational motion; elementary-particle rotations, on the other hand, are highly nonadiabatic, due to their small masses, and distortions of the rotating system can be large enough to overwhelm the effect of the conventional centrifugal barrier.

---

*Work performed under the auspices of the U. S. Energy Research and Development Administration under Contract No. W-7405-Eng-48.

[1]The quantum numbers of the $\psi(3095)$ or J particle are taken from A. M. Boyarski *et al.*, Phys. Rev. Lett. 34, 1357 (1975). The lifetime of the ψ, which is calculated from the width value $\Gamma_\psi = 69 \pm 15$ keV, is an upper limit, since a (small) partial decay mode to undetected neutrals may exist.

[2]The quantum numbers of the $\psi'(3684)$ particle are taken from V. Lüth *et al.*, Phys. Rev. Lett. 35, 1124 (1975).

[3]W. Braunschweig *et al.*, Phys. Lett. 57B, 407 (1975); G. J. Feldman *et al.*, *ibid.* 35, 821 (1975).

[4]M. L. Perl *et al.*, Phys. Rev. Lett. 35, 1489 (1975); also see a theoretical paper by A. De Rújula *et al.*, *ibid.* 35, 628 (1975).

[5]K. Niu *et al.*, Prog. Theor. Phys. 46, 1644 (1971); H. Sugimoto *et al.*, *ibid.* 53, 1541 (1975); A. Benvenuti *et al.*, Phys. Rev. Lett. 34, 419 (1975); M. R. Krishnaswamy *et al.*, Phys. Lett. 57B, 105 (1975); E. G. Cazzoli *et al.*, Phys. Rev. Lett. 34, 1125 (1975) [but see A. Benvenuti *et al.*, Phys. Rev. Lett. 35, 1486 (1975)].

[6]Particle Data Group, Phys. Lett. 50B, 1 (1974) (referred to here as RPP74).

[7]For an example of a mass calculation, see M. H. Mac Gregor, Phys. Rev. D 12, 1492 (1975).

[8]A. Browman *et al.*, Phys. Rev. Lett. 32, 1067 (1974).

[9]A. Duane *et al.*, Phys. Rev. Lett. 32, 425 (1974). The η' lifetime value shown in Table I of the present paper was obtained by fitting parabolas to the two sets of data in Table I of Duane *et al.* and averaging the results; the error limit quoted here is an average of the $\Delta\chi^2 = +1$ values obtained from these two parabolas.

[10]Although the Σ^0 lifetime quoted in Ref. 6 is just an upper limit, this upper limit is about the value expected from the present systematics.

[11]A. Browman *et al.*, Phys. Rev. Lett. 33, 1400 (1974).

[12]B. T. Feld, *Models of Elementary Particles* (Blaisdell, Waltham, 1969), Sec. 7.4.

[13]For example, the lifetimes of the electromagnetically inhibited η meson and the strongly decaying ω meson occur in the ratio $\tau_\eta \simeq \tau_\omega \times \alpha^{-2}$.

[14]M. H. Mac Gregor, in *Fundamental Interactions at High Energies*, proceedings of the 1971 Coral Gables Conference, edited by M. Dal Cin, G. J. Iverson, and A. Perlmutter (Gordon and Breach, New York, 1971), Vol. 3, p. 75; Nuovo Cimento 8A, 235 (1972); 20A, 471 (1974); Phys. Rev. D 9, 1259 (1974), Sec. XII.

[15]The short-lived resonances include all resonances in RPP74, Ref. 6, except those of Table I in the present paper, which have quoted lifetime or width values. In cases where a spread of values is given, the RPP74 quoted average was used where available. In some cases where different charge states of a resonance have separately quoted lifetimes, both of these lifetimes were included. In Figs. 5 and 6, the abscissa corresponds to the lifetime logarithms X as obtained from Eq. (2), and the ordinate gives an equally spaced distribution of the logarithms X after they have been sorted out into $\Delta X = 0.1$ bins.

[16]We ordinarily expect a resonance to exhibit the same mass and the same observed total width in all of its decay modes. However, both the observed mass and the observed width for a particular decay mode can be shifted if there is a severe phase-space constraint which occurs for just this specific decay mode. The ϕ meson is the only example known to the author in which this condition occurs. The $\phi \to KK$ decay mode, which has been used for most experimental determinations of the ϕ-meson parameters, is highly unusual in that it is a spin-1 decay with a very small Q value. From the Q value of 30 MeV, each final-state kaon has a kinetic energy of only 15 MeV, or a linear momentum of 123 MeV/c. Thus, in order to carry away the spin-1 angular momentum of the ϕ, the two kaons must have a noncollinear separation distance of 2.3 F. If we assume that the 1019-MeV ϕ meson has about the same "size" as the measured size of the 939-MeV nucleon, this large separation distance required for the final-state kaons constitutes a severe kinematic constraint, and it limits the available phase space for the decay by cutting off the low-momentum portion, thus increasing the observed mass of the ϕ in this decay channel and decreasing its observed width. The ϕ in its $\phi \to \pi\pi\pi$ decay mode does not have this severe kinematic constraint, and it appears in some experiments at a lower mass and with an apparently broader width [see M. Aguilar-Benitez *et al.*, Phys. Rev. D 9, 29 (1971), Fig. 61 and the accompanying discussion; J.-E. Augustin *et al.*, Phys. Lett. 28B, 517 (1969); G. R. Kalbfleisch *et al.*, Phys. Rev. D 13, 22 (1976), which would place it closer to the "resonance region" of Fig. 5 in the present paper. However, in Orsay Storage Ring experiments [G. Cosme *et al.*, Phys. Lett. 48B, 155 (1974); G. Parrour *et al.*, Orsay Report No. LAL 1280, 1975 (unpublished)], the $e^+e^- \to \phi \to 3\pi$ and $e^+e^- \to \phi \to K_L^0 K_S^0$ measurements of the ϕ mass and width give very similar results.

[17]See M. H. Mac Gregor, Lett. Nuovo Cimento 1, 759 (1971).

[18]L. Gray *et al.*, Phys. Rev. Lett. 26, 1491 (1971); L. Gray *et al.*, Phys. Rev. Lett. 30, 1091 (1973).

[19]This result is in agreement with a light-quark approach to hadron spectroscopy; see M. H. Mac Gregor, Phys. Rev. D 10, 850 (1974).

[20]For a calculation of the neutron to muon lifetime that does not depend on α, see J. Bernstein, *Elementary Particles and Their Currents* (Freeman, San Francisco, 1968), p. 128. The present results would seem to call into question the validity of this current-algebra lifetime calculation.

[21]Statistically speaking, the appearance of accurate 1:2:4 ratios in the lifetime suggests the existence of 4:2:1 resonance decay triggers (light-quark substates), whose spontaneous and independent annihilations can initiate the over-all particle decays [see M. H. Mac Gregor, Ref. 19, Fig. 23].

[22]B. T. Feld, *Models of Elementary Particles* (Ref. 12), Chap. IV.

[23]G. Källén, *Elementary Particle Physics*, (Addison-Wesley, Reading, Mass., 1964).

[24]V. Vuillemin *et al.*, Nuovo Cimento Lett. 14, 165 (1975).

[25]W. Blum *et al.*, Phys. Lett. 57B, 403 (1975).

[26]See M. Deutschmann *et al.*, Nucl. Phys. B61, 102 (1973), Fig. 6.